Corannulenes

Deutsche Ausgabe: DOI: 10.1002/ange.201608337
Internationale Ausgabe: DOI: 10.1002/anie.201608337

Pentaindenocorannulene: Properties, Assemblies, and C_{60} Complex

Samuel Lampart, Loïc M. Roch, Amit K. Dutta, Yujia Wang, Rangana Warshamanage, Aaron D. Finke, Anthony Linden, Kim K. Baldridge, and Jay S. Siegel**

Abstract: *Pentaindenocorannulene ($C_{50}H_{20}$, **1**), a deep bowl polynuclear aromatic hydrocarbon, accepts 4 electrons, crystallizes in columnar bowl-in-bowl assemblies and forms a nested C_{60}@**1**$_2$ complex. Spectra, structures and computations are presented.*

Curved polynuclear aromatic hydrocarbons (PAH) of the type $C_{10n}H_{10}$ ($n = 2$–5) undergo a transition from bowls to capped tubes (Figure 1),[1] in which optoelectronic properties vary with degree of bowl/cap curvature and π-surface area.[2] A related PAH, pentaindenocorannulene ($C_{50}H_{20}$, **1**)[3] displays a cap curvature similar to $C_{30}H_{10}$ (hub POAV[4] = 12.4° $C_{30}H_{10}$ vs. 12.6° **1**)[1,2] with the additional feature of five benzo-fingers that create a substantial π-surface area as well as greater bowl depth and volume. The molecular structure of **1** creates material expectations such as low HOMO–LUMO gap, ease of reduction and higher order supramolecular assemblies.[5]

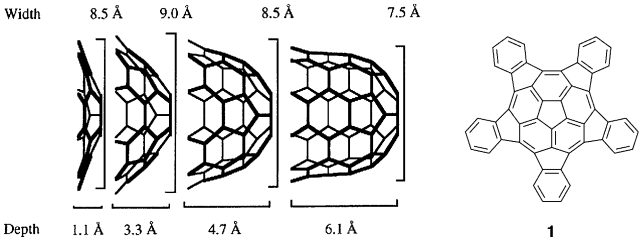

Figure 1. $C_{10n}H_{10}$ ($n = 2$–5) and pentaindenocorannulene **1**.

An elegant synthesis of **1** is reported to proceed in three steps from corannulene,[3] with the ultimate step involving a five-fold palladium-mediated cyclization carried out in a microwave reactor at maximum power, 180 °C over 45 minutes. In our hands, it was necessary to run the reaction without using the maximum power option, but at a higher temperature, 200 °C, and for shorter time, 15 min (Scheme 1). These conditions yielded robustly 20–30 % of **1** on mg scale across several microwave reactors in Zurich as well as in Tianjin, and, by iterative implementation produced several hundred mg of **1**.[6]

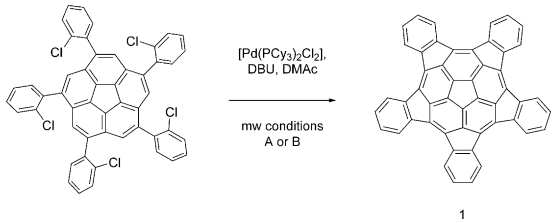

Scheme 1. Synthesis of **1**. Conditions A: 180 °C, power max, 45 min, 35 %; conditions B: 200 °C, power 300 W, 15 min, 20–30 %.

Crystals of a minor impurity, **2** (Figure 2), were isolated and revealed to be from an oxidative cleavage of the corannulene subunit rim CC bond. **2** could form via palladium C–C insertion into the strained bond followed by incorporation of oxygen, thus highlighting C–C insertion as a deleterious side reaction and a new mode for selective bowl reactivity.[7]

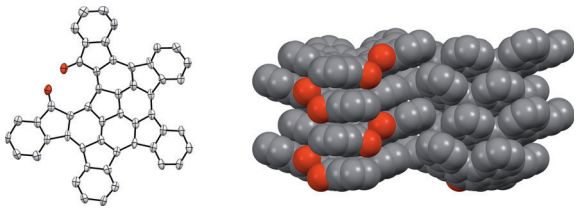

Figure 2. Structure of oxidized impurity **2**.

Cyclic voltammetry of **1** displayed four reversible reduction waves (Figure 3),[8] consistent with expectations based on previous studies of compounds with extended π-surfaces and increased bowl-curvature.[9] The first reduction potential of **1** is lower by ca. 0.6 V (in THF) compared to monoindenocorannulene, and by ca. 1 V compared to corannulene, consistent with a curvature-stabilized LUMO.

The UV-vis spectrum of **1** in 2-methyltetrahydrofuran (MeTHF) exhibits absorptions around 295 and 374 nm with a tailing that extends above 500 nm (Figure 4). The emission of **1** (MeTHF) was measured at RT with excitation at 374 nm, and revealed a broad maximum at about 580 nm (530–680 nm). The RT fluorescence quantum yield for **1** is 3.06 % (oDCB) with a lifetime of 4.8 ns in tetrachloroethane (TCE).

[*] Dr. S. Lampart, L. M. Roch, Dr. A. K. Dutta, Prof. Dr. A. Linden, Prof. Dr. K. K. Baldridge, Prof. Dr. J. S. Siegel
Department of Chemistry, University of Zurich
Winterthurerstrasse 190, 8057 Zurich (Switzerland)
E-mail: kimb@chem.uzh.ch
Dr. A. K. Dutta, Y. Wang, Prof. Dr. K. K. Baldridge, Prof. Dr. J. S. Siegel
School of Pharmaceutical Science and Technology, Tianjin University
92 Weijin Road, Nankai District, Tianjin-3000072 (China)
E-mail: dean_spst@tju.edu.cn
Dr. R. Warshamanage, Dr. A. D. Finke
Swiss Light Source, Paul Scherrer Institute
5232 Villigen (Switzerland)

Supporting information for this article can be found under: http://dx.doi.org/10.1002/anie.201608337.

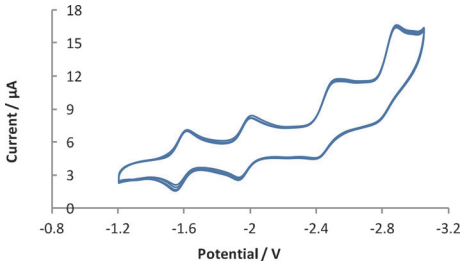

Figure 3. Exptl [B97-3/Def2-TZVPD(THF)//B97-D/6-311G(2d,p) calcd] reduction potentials of **1** in THF and corrected to Fc/Fc^{+} (+0.085 V): −1.58 [−1.56], −1.96 [−2.03], −2.45 [−2.39], and ca. −2.9 [−2.80] V.

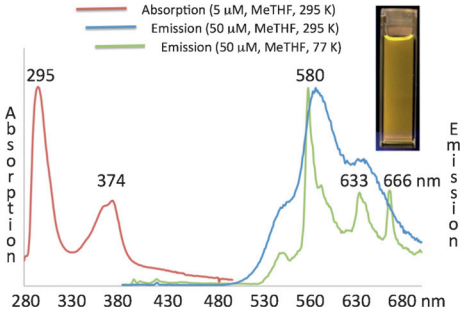

Figure 4. UV-vis absorption and emission spectra (excitation 374 nm).

Absorption, excitation and emission spectra are invariant to concentration in the range 1–50 µM (Figure SI.4 in the Supporting Information). Measurements at −196 °C in a MeTHF glass matrix displayed a fluorescence lifetime of 8.2 ns and better resolution of the vibrational fine structure (ca. 1400 cm^{-1}) accountable to modes of the aromatic rings. A new peak at 666 nm could derive from the onset of phosphorescence at −196 °C. Coincidentally, C_{70} shows a fluorescence manifold (640–710 nm) along with a longer lived phosphorescence (790–950 nm); hinting that the similar curvature could connect the properties of fullerenes and **1**.[1,10]

The ^{1}H NMR spectrum of **1** showed a substantial concentration dependence in the range 2–800 µM (TCE-d_2) (Figure 5; Figures SI.1–SI.3). Varying the temperature also showed changes in the ^{1}H NMR spectrum, such that lower temperature and increase in concentration resulted in similar

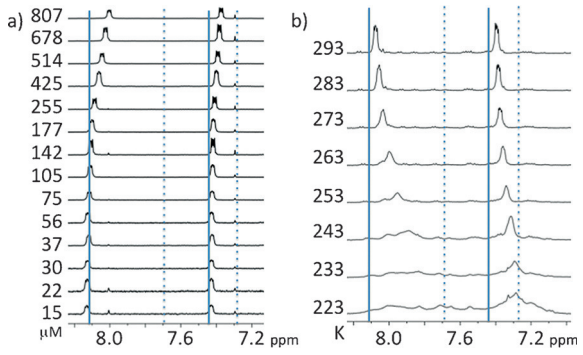

Figure 5. ^{1}H NMR of **1**: a) Variable concentration, 15–807 µM; b) variable temperature, 223–293 K. Blue lines are computationally predicted values, monomer: solid lines; dimer: dotted lines.

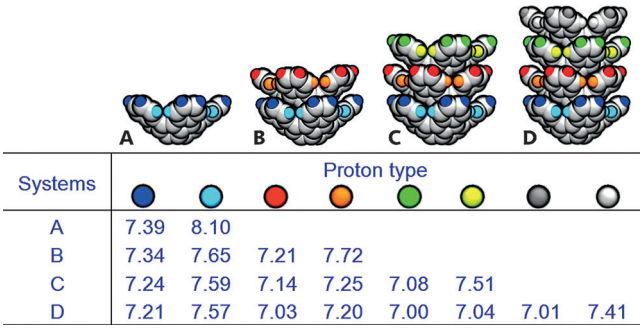

Systems	Proton type							
A	7.39	8.10						
B	7.34	7.65	7.21	7.72				
C	7.24	7.59	7.14	7.25	7.08	7.51		
D	7.21	7.57	7.03	7.20	7.00	7.04	7.01	7.41

Figure 6. CSGT/B97-D/Def2-TZVP//B97-D/6–311G(2d,p) determined chemical shifts in TCE for computed complexes (**A** = **1**, **B** = $\mathbf{1}_2$, **C** = $\mathbf{1}_3$, **D** = $\mathbf{1}_4$). Colors correspond to specific sets of C_{5v} symmetry-unique hydrogen atoms.

spectroscopic shifts. This behavior hinted that **1** aggregates in solution. A serial dilution study arrived at an asymptotic limit of 7.43 ppm and 8.13 ppm.

Figure 6 summarizes the CSGT/B97-D/Def2-TZVP//B97-D/6-311G(2d,p) determined ^{1}H chemical shielding tensor in TCE for monomer **1.** The results are in line with the experimental observation at low concentration. The shifts of the two C_{5v} symmetry unique H atoms in **1** are 7.43 [7.39, blue] ppm and 8.13 [8.10, cyan] ppm, exptl [calcd] (Figure 6). Chemical shifts for the static dimer of **1** are shielded compared to those of the monomer.[11] Assuming a dynamically exchanging dimer, the computational values predict ^{1}H NMR shifts for the dimer to be 7.28 and 7.69 ppm. The spectrum at the low temperature limit (−30 to −40 °C) approaches values of 7.3 ppm and 7.9 ppm before broadening extremely. By comparison, a room temperature saturated solution of **1** in TCE shows values of 7.95 and 7.35 ppm. From these observations and the predicted ^{1}H NMR values, the dimer association constant must be on the order of 10^{3}–10^{4};[12] and, if the broadening of the proton signals between −53 and −33 °C is attributed to slow exchange, then a barrier for the exchange process would be on the order of 11–12 kcal mol^{-1}.[13]

Dimer formation is consistent with the toluene solvate structure reported for **1**, which showed a series of dimers stacked in a herringbone fashion.[3] Crystals of **1** (0.03 × 0.06 × 0.10 mm) grown from bromoform produced a solvate that required synchrotron radiation for the resolution of the structure (Figure 7). In this case, molecules of **1** stack into infinite bowl-in-bowl columns, similar to the packing motif found for other curved PAHs.[3b,14] The bowl-stacks face in opposite directions in adjacent columns resulting in a centrosymmetric space group. The bowl centroid–bowl centroid distances along the columns range from 3.560(3) to 3.645(3) Å, approximately the arene π–π van der Waals distance. Within each column, molecules $n-1$, n, $n+1$ etc. are rotated 36° about the column axis leading to a staggered type of stacking. A staggered conformation was also observed for the dimers of the toluene solvate of **1**,[3] showcasing the propensity of **1** to form ordered aggregates.

B97-D/Def2-TZVP//B97-D/6-311G(2d,p) calculations in dichlorobenzene on monomer through tetramer of **1** served as

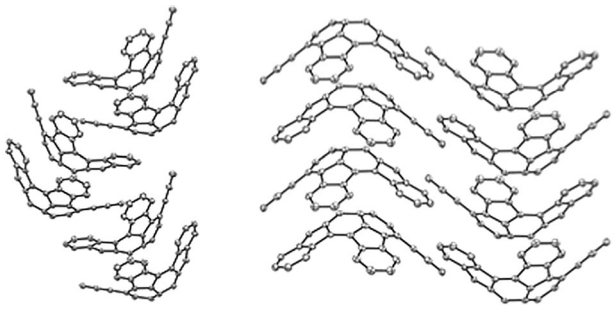

Figure 7. Crystal packing motifs of **1**. Left: toluene solvate; right: bromoform solvate. Hydrogen atoms and solvent of crystallization are omitted.

a model for comparison of the energetics of various crystal unit cell geometries. Staggered and eclipsed arrangements were considered and it was determined that, in all cases, a 36° rotation between each unit along the stacking axis was favored. Each eclipsed alignment between two units leads to a destabilization of 5–6 kcal mol^{-1}, regardless of the number of total units. Comparison of **1** as a column of four bowls (analogous to the infinite stack polymorph) vs. the dimer of dimer (analogous to the herring bone dimer polymorph) favors the columnar form by ca. 8.5 kcal mol^{-1}, as illustrated in Figure 8.[15]

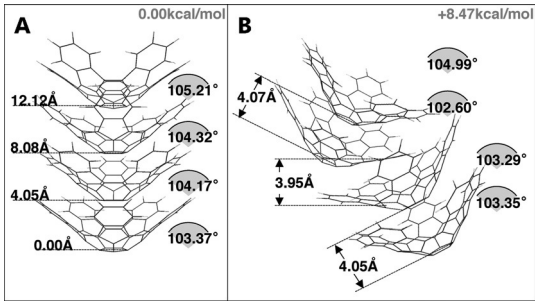

Figure 8. B97-D/Def2-TZVP(dichlorobenzene)//B97-D/6-311G(2d,p) calculated tetramers of **1**: A) columnar, B) herringbone. Bowl-to-bowl distances between subunits and the bowl angles are shown.

Given the substantial concave-convex surface recognition among molecules of **1**, it is reasonable to anticipate that the concave surface of **1** might recognize fullerene convex surfaces.[5] Evidence for C_{60} corannulene in the gas phase[16] was followed by observation of a ball-in-bowl assembly on copper corannulene C_{60} surfaces,[17] and a crystalline C_{60} corannulene complex.[18] Corannulene has been a structural element in various "bucky catcher" molecules;[19,20] and related curved aromatics[21] form inclusion complexes with C_{60}. The interaction of fullerenes with **1** should be stronger.

Evidence for a potential C_{60}@**1** complex in solution came from the method of continuous variations (Job plot, Figure SI.6)[22] applied to the ^{1}H NMR chemical shifts of different molar fractions of C_{60} and **1** at a constant total concentration of 2 mM. The concentration range was at the solubility limit of **1**. The data suggest formation of a complex between C_{60} and **1**; the maximum of 0.68 indicates a 1:2 stoichiometry (C_{60}@$\mathbf{1}_2$).

UV-vis spectroscopy did not show any new absorption bands for the aggregate (Figures SI.8 and SI.9); however, titration of a solution of **1** (10 μM in TCE) with C_{60} (TCE) showed fluorescence quenching (Figure 9a). A Stern–Volmer plot ($F°/F$ vs. [C_{60}]; Figure 9b)[23] of the titration data fit well to a line (slope 1.7×10^4) and the fluorescence lifetime was unperturbed ($\tau_0/\tau = 1$), consistent with quenching caused by the C_{60}@**1** complex. Deviations from linearity occur when [**1**] $>$ 100 μM, suggestive of higher aggregation.

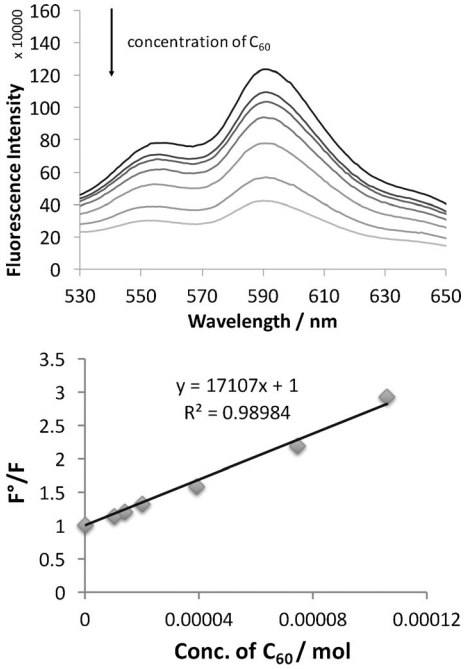

Figure 9. Upper panel: Fluorescence quenching of **1** by titration with C_{60}. Lower panel: Stern–Volmer plot.

A sample of **1** and C_{60} in the molar ratio of 2:1 (oDCB) was analyzed by high-resolution atmospheric pressure chemical ionization mass spectrometry (HR-APCI-MS). Besides the dominant peaks of the two individual substrates, the ionic adducts $[\mathbf{1}_2]+H^+$, $[C_{60}@\mathbf{1}]+H^+$ and $[C_{60}@\mathbf{1}_2]+H^+$ were detected (Figures SI.10 and SI.11).

Crystals of the complex were obtained from a TCE solution. Synchrotron radiation was needed to resolve the structure of the tiny crystals ($0.01\times0.04\times0.06$ mm). The crystallographic analysis revealed a trimeric complex C_{60}@$\mathbf{1}_2$ in which the C_{60} was found to be complexed to the concave face of $\mathbf{1}_2$ as a staggered *nested* dimer rather than *sandwiched* between two individual **1** molecules (Figure 10). With regard to the C_{60}@$\mathbf{1}_2$ units, no continuous stacking is present. The co-crystallized solvent molecules and the C_{60} molecules were heavily disordered, rendering the overall quality and precision of the result rather low ($R = 0.19$). Hence, analysis of the geometrical parameters should be avoided. Nevertheless, it is possible to distinguish convex-concave π–π interactions between C_{60} and **1** as well as between **1** molecules.

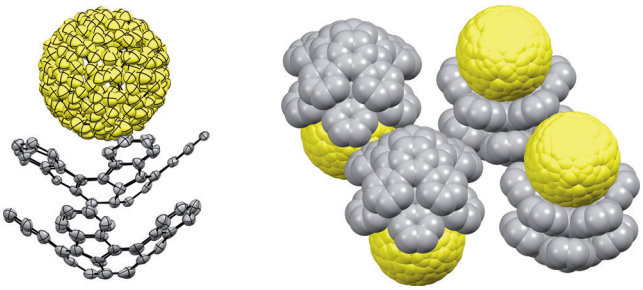

Figure 10. Asymmetric unit of the crystal structure of the complex C_{60}@**1**$_2$ (left) and its packing motif (right).

B97-D/Def2-TZVP//B97-D/6-311G(2d,p) computations in oDCB for C_{60}@**1**$_n$ aggregates suggest a clear preference (ca. 3.5 kcal mol^{-1}) for staggered over eclipsed conformations, with regard to the hub rings of **1** and C_{60}. Of 2:1 aggregate configurations—"nest" C_{60}@**1**$_2$, and "sandwich" **1**(C_{60})**1**—the nest configuration, found crystallographically, is favored by ca. 11.5 kcal mol^{-1} (Figure 11 A and B, respectively). C_{70}@**1** and C_{70}@**1**$_2$ were investigated in a similar way for comparison; the structures and energetics parallel the C_{60}@**1**$_n$ aggregates (Figure 11 C and D).

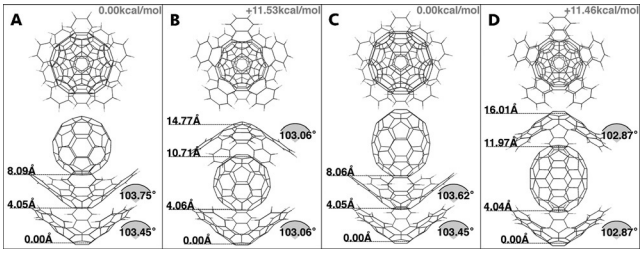

Figure 11. B97D/Def2-TZVP//B97-D/6-311G(2d,p) calculated structures in dichlorobenzene of C_{60}@**1**$_2$ (A and B) and C_{70}@**1**$_2$ (C and D); "nested" (A and C) vs. "sandwiched" (B and D) configuration.

In summary, a modification of the original synthesis enables robust preparation of over 100 mg of **1**. Cyclic voltammetry shows that **1** has a reversible multi-electron reduction profile (−1.58 eV, 1st reduction). NMR and MS data suggest that **1** is prone to form dimers and higher assemblies in solution, and the isolation of a bromoform solvate reveals columnar stacks of **1** in the solid state. Evidence for C_{60}@**1**$_n$ complexes was presented in solution and in the solid state, and was modeled theoretically. Control of the competition between formation of assemblies of **1** and C_{60}@**1**$_n$ aggregation should lead to stronger and more selective fullerene@bowl complexes.

Experimental Section

Synthesis of **1**: To a 10 mL microwave tube was added 1,3,5,7,9-pentakis(2-chlorophenyl)corannulene (20.0 mg, 0.025 mmol), [$PdCl_2$-(PCy_3)$_2$] (16.7 mg, 0.023 mmol), and DMAc (3 mL). To the yellow suspension DBU (0.14 mL, 0.936 mmol) was given, and the microwave tube was sealed with its cap. The mixture was irradiated with microwaves at 200 °C for 15 min (microwave limit settings: 200 °C, 300 W without max power, 15 bar; reaction values: 200 °C, 40 W on average, 1–3 bar on average). The deep red reaction mixture was allowed to cool to room temperature, was then transferred to a vial with CH_2Cl_2 (2 mL), and was allowed to stand for 2 h. Intense orange crystals of pentaindenocorannulene were observed within the crude mixture. Purification by flash chromotography (silica gel, $CHCl_3$) afforded the desired product as an intense orange solid (3 mg, 0.005 mmol) in 19 % yield. NMR data in agreement with reported data.[3a]

CCDC 1499785, 1499786 and 1499787 contain the supplementary crystallographic data for this paper. These data can be obtained free of charge from The Cambridge Crystallographic Data Centre via www.ccdc.cam.ac.uk/structures.

Computational details: B97-D[24]/Def2-TZVP[25]//B97-D/6-311G-(2d,p)[26] density functional theory was used for all structure, energetics (in oDCB solvent), and associated Hessian analyses. ^{1}H chemical shielding tensor data employed the CSGT[27]/B97-D/Def2-TZVP(TCE)//B97-D/6-311G(2d,p), and data referenced using a calibration scheme.[28] Reduction potential data employed B97-3[29]/Def2-TZVPD(THF)//B97-D/6-311G(2d,p) with $E° = -\Delta E$/nF, $n = 1$, F = 1 eV, referenced to Ag/AgCl. Effects of solvent employed the COSMO:ab initio continuum method.[30] Further details in the Supporting Information.

Acknowledgements

We thank the Swiss National Science Foundation, National Basic Research Program of China (2015CB856500), the Qian Ren Scholar Program of China, and the Synergetic Innovation Center of Chemical Science and Engineering (Tianjin) for supporting this work.

Keywords: C_{60} · corannulenes · cyclic voltammetry · dynamic NMR spectroscopy · polycyclic aromatic hydrocarbons

How to cite: *Angew. Chem. Int. Ed.* **2016**, *55*, 14648–14652
Angew. Chem. **2016**, *128*, 14868–14872

[1] K. K. Baldridge, J. S. Siegel, *Theor. Chem. Acc.* **1997**, *97*, 67.
[2] Reviews on curved PAHs: a) Y.-T. Wu, J. S. Siegel, *Chem. Rev.* **2006**, *106*, 4843; b) V. M. Tsefrikas, L. T. Scott, *Chem. Rev.* **2006**, *106*, 4868; c) L. Zoppi, J. S. Siegel, K. K. Baldridge, *WIREs Comput. Mol. Sci.* **2013**, *3*, 1; d) Y.-T. Wu, J. S. Siegel, *Top. Curr. Chem.* **2014**, *349*, 63.
[3] a) E. A. Jackson, B. D. Steinberg, M. Bancu, A. Wakamiya, L. T. Scott, *J. Am. Chem. Soc.* **2007**, *129*, 484; b) A. S. Filatov, L. T. Scott, M. A. Petrukhina, *Cryst. Growth Des.* **2010**, *10*, 4607; c) B. D. Steinberg, E. A. Jackson, A. S. Filatov, A. Wakamiya, M. A. Petrukhina, L. T. Scott, *J. Am. Chem. Soc.* **2009**, *131*, 10537.
[4] a) R. C. Haddon, L. T. Scott, *Pure Appl. Chem.* **1986**, *58*, 137; b) R. C. Haddon, *Acc. Chem. Res.* **1988**, *21*, 243.
[5] a) P. A. Denis, *Chem. Phys. Lett.* **2014**, *591*, 323; b) P. A. Denis, *Chem. Phys. Lett.* **2011**, *516*, 82.
[6] The occasion was utilized to test alternatives to the published route to **1**. However, neither C–F activation by silylium ions[31] nor by activated aluminum oxide[32] affected the conversion of 1,3,5,7,9-pentakis(2-fluorophenyl)corannulene to the target.
[7] Structure and spectra are given in the Supporting Information.
[8] Because the anionic peak potential of the fourth peak was not distinct enough, only three reduction potentials were quantified.
[9] a) A. K. Dutta, A. Linden, L. Zoppi, K. K. Baldridge, J. S. Siegel, *Angew. Chem. Int. Ed.* **2015**, *54*, 10792; *Angew. Chem.* **2015**, *127*,

10942; b) T. J. Seiders, K. K. Baldridge, R. Gleiter, J. S. Siegel, *Tetrahedron Lett.* **2000**, *41*, 4519; c) C. Bruno, R. Benassi, A. Passalacqua, F. Paolucci, C. Fontanesi, M. Marcaccio, E. A. Jackson, L. T. Scott, *J. Phys. Chem. B* **2009**, *113*, 1954.

[10] S. M. Argentine, A. H. Francis, C.-C. Chen, C. M. Lieber, J. S. Siegel, *J. Phys. Chem.* **1994**, *98*, 7350 – 7354.

[11] The chemical shifts of the second bowl from the bottom of systems **B**, **C** and **D** converge such that in system **D** red vs. green and orange vs. lime hydrogens show similar chemical shifts.

[12] $2A \rightarrow A_2$; $K = [A_2]/[A][A]$; if $[A] = [A_2]$ then $K = 1/[A]$, see: K. A. Connors, *Binding Constants: The Measurement of Molecular Complex Stability*, Wiley, New York, **1987**.

[13] Approximation $\Delta G^{\ddagger} = T_c/20$ for $10\,\text{Hz} < \Delta\nu < 50\,\text{Hz}$: see: J. Sandstrom, *Dynamic NMR Spectroscopy*, Academic Press, New York, **1982**.

[14] a) A. Sygula, H. E. Folsom, R. Sygula, A. H. Abdourazak, Z. Marcinow, R. Fronczek, P. W. Rabideau, *J. Chem. Soc. Chem. Commun.* **1994**, 2571; b) D. M. Forkey, S. Attar, B. C. Noll, R. Koerner, M. M. Olmstead, A. L. Balch, *J. Am. Chem. Soc.* **1997**, *119*, 5766; c) M. A. Petrukhina, K. W. Andreini, L. Peng, L. T. Scott, *Angew. Chem. Int. Ed.* **2004**, *43*, 5477; *Angew. Chem.* **2004**, *116*, 5593; d) H. Sakurai, T. Daiko, H. Sakane, T. Arnaya, T. Hirao, *J. Am. Chem. Soc.* **2005**, *127*, 11580; e) J. G. Brandenburg, S. Grimme, P. G. Jones, G. Markopoulos, H. Hopf, M. K. Cyranski, D. Kuck, *Chem. Eur. J.* **2013**, *19*, 9930.

[15] A study of a series of indenocorannulene crystal structures revealed offset columnar stacks except for **1**,[3b] where, despite potential strong dipole alignment and large van der Waals surface overlap benefits for columnar stacking, the herringbone arrangement of dimers was observed. The authors conclude that CH-to-π interactions must therefore dominate and control the packing order; however, the bromoform solvate of **1** and tetramer computations support an axially aligned columnar stacking as the most stable form. The herringbone arrangement of dimers is a meta-stable form and conclusions about strong CH-to-π interactions are pure speculation.

[16] H. Becker, G. Javahery, S. Petrie, P. C. Cheng, H. Schwarz, L. T. Scott, D. K. Bohme, *J. Am. Chem. Soc.* **1993**, *115*, 11636.

[17] W. Xiao, D. Passerone, P. Ruffieux, K. Ait-Mansour, O. Grönig, E. Tosatti, J. S. Siegel, R. Fasel, *J. Am. Chem. Soc.* **2008**, *130*, 4767.

[18] L. N. Dawe, T. A. AlHujran, H.-A. Tran, J. I. Mercer, E. A. Jackson, L. T. Scott, P. E. Georghiou, *Chem. Commun.* **2012**, *48*, 5563 – 5565.

[19] a) S. Mizyed, P. E. Georghiou, M. Bancu, B. Cuadra, A. K. Rai, P. C. Cheng, L. T. Scott, *J. Am. Chem. Soc.* **2001**, *123*, 12770; b) P. E. Georghiou, A. H. Tran, S. Mizyed, M. Bancu, L. T. Scott, *J. Org. Chem.* **2005**, *70*, 6158; c) A. Sygula, F. R. Fronczek, R. Sygula, P. W. Rabideau, M. M. Olmstead, *J. Am. Chem. Soc.* **2007**, *129*, 3842 – 3843; d) V. H. Le, M. Yanney, M. McGuire, A. Sygula, E. A. Lewis, *J. Phys. Chem. B* **2014**, *118*, 11956 – 11964; e) M. Yanney, F. R. Fronczek, A. Sygula, *Angew. Chem. Int. Ed.* **2015**, *54*, 11153 – 11156; *Angew. Chem.* **2015**, *127*, 11305 – 11308; f) P. L. Abeyratne Kuragama, F. R. Fronczek, A. Sygula, *Org. Lett.* **2015**, *17*, 5292 – 5295.

[20] Reviews on fullerene hosts: a) T. Kawase, H. Kurata, *Chem. Rev.* **2006**, *106*, 5250; b) E. M. Pérez, N. Martin, *Chem. Soc. Rev.* **2008**, *37*, 1512; c) D. Canevet, E. M. Pérez, N. Martin, *Angew. Chem. Int. Ed.* **2011**, *50*, 9248; *Angew. Chem.* **2011**, *123*, 9416.

[21] a) H. Yokoi, Y. Hiraoka, S. Hiroto, D. Sakamaki, S. Seki, H. Shinokubo, *Nat. Commun.* **2015**, *6*, 8215; b) B. T. King, M. M. Olmstead, K. K. Baldridge, B. Kumar, A. L. Balch, J. A. Gharamaleki, *Chem. Commun.* **2012**, *48*, 9882.

[22] a) P. Job, *Ann. Chim.* **1928**, *9*, 113; b) J. S. Renny, L. L. Tomasevich, E. H. Tallmadge, D. B. Collum, *Angew. Chem. Int. Ed.* **2013**, *52*, 11998; *Angew. Chem.* **2013**, *125*, 12218.

[23] J. R. Lakowicz, *Principles of Fluorescence Spectroscopy*, Springer, New York, **2006**.

[24] S. Grimme, *J. Comput. Chem.* **2006**, *27*, 1787.

[25] F. Weigend, R. Ahlrichs, *Phys. Chem. Chem. Phys.* **2005**, *7*, 3297.

[26] K. Raghavachari, J. S. Binkley, R. Seeger, J. A. Pople, *J. Chem. Phys.* **1980**, *72*, 650.

[27] T. A. Keith, R. F. W. Bader, *Chem. Phys. Lett.* **1993**, *210*, 223.

[28] K. K. Baldridge, J. S. Siegel, *J. Phys. Chem. A* **1999**, *103*, 4038.

[29] T. W. Keal, D. J. Tozer, *J. Chem. Phys.* **2005**, *123*, 121103.

[30] a) K. K. Baldridge, A. Klamt, *J. Chem. Phys.* **1997**, *106*, 6622; b) A. Klamt, G. Schürmann, *J. Chem. Soc. Perkin Trans. 2* **1993**, 799.

[31] O. Allemann, S. Duttwyler, P. Romanato, K. K. Baldridge, J. S. Siegel, *Science* **2011**, *332*, 574 – 577.

[32] a) K. Y. Amsharov, P. Merz, *J. Org. Chem.* **2012**, *77*, 5445 – 5448; b) K. Y. Amsharov, M. A. Kabdulov, M. Jansen, *Angew. Chem. Int. Ed.* **2012**, *51*, 4594 – 4597; *Angew. Chem.* **2012**, *124*, 4672 – 4675.

Received: August 25, 2016
Published online: October 6, 2016

